

## Enhanced Stability of Electrohydrodynamic Jets through Gas Ionization

Sibel Korkut, Dudley A. Saville,\* and Ilhan A. Aksay†

*Department of Chemical Engineering, Princeton University, Princeton, New Jersey 08544-5263, USA*  
(Received 4 July 2007; revised manuscript received 5 November 2007; published 25 January 2008)

Theoretical predictions of the nonaxisymmetric instability growth rate of an electrohydrodynamic jet based on the measured total current overestimate experimental values. We show that this apparent discrepancy is the result of gas ionization in the surrounding gas and its effect on the surface charge density of the jet. As a result of gas ionization, a sudden drop in the instability growth rate occurs below a critical electrode separation, yielding highly stable jets that can be used for nano- to microscale printing.

DOI: [10.1103/PhysRevLett.100.034503](https://doi.org/10.1103/PhysRevLett.100.034503)

PACS numbers: 47.65.-d, 47.85.Dh, 52.80.-s, 68.03.-g

Electrohydrodynamic (EHD) jets [1] emitted from liquid cones undergo various modes of instabilities [2,3] which cause them to break into droplets or whip before reaching the opposite electrode. The droplet formation and the whipping phenomenon have been utilized in many technologically important applications including electro-spraying [4] and electrospinning [5]. A most recent trend has been on printing with the liquid jet [6–13] nano- to micrometer size features when the whipping instability disappears while the counter electrode is in close proximity of the nozzle. Although the stability of EHD jets has been the subject of various studies [14–16] and the jet behavior can be predicted qualitatively, experimental conditions leading to the disappearance of the whipping instability are not understood. Theoretical calculation of instability growth rate requires surface charge density of the jet which is estimated based on measured total current between the two electrodes [17,18]. Using such an estimation of surface charge density in the calculations leads to overestimation of the experimental instability growth rates by several orders of magnitude raising doubts on the validity of the existing theories. In other words, the EHD jets travel a much longer length than what is expected by the theoretical predictions before the whipping instability sets in. This observation was first made by Taylor as early as 1969 without a satisfactory explanation [2].

For printing with the liquid jet, it is crucial to provide a fundamental explanation for this discrepancy so that the conditions leading to high resolution printing can be predicted reliably. In this Letter, we show that this apparent discrepancy between theory and the experiments is due to the ionization of the gas surrounding the jet, which was observed by the electro-spraying community [19–22] but was never related to the whipping instability because of the early jet break up. When the effects of gas ions are not taken into account, the total measured current leads to an inaccurate estimation of surface charge density of the jet, which causes the calculated instability growth rates to be large. A beneficial consequence of gas discharge at close proximity of the electrodes is the enhanced stability of the jet as its charge density is reduced.

We performed our experiments with stainless steel ( $13 \times 13$  cm) parallel plate electrodes. The upper electrode had a stainless steel nozzle with a  $640 \mu\text{m}$  outer diameter protruding 2 mm below its surface and the lower electrode had a 15 mm diameter hole at its center that was connected to a small reservoir underneath. The setup was enclosed inside a Plexiglas chamber and the humidity level was regulated by feeding a saturated stream of nitrogen gas which bubbled through water kept at  $60^\circ\text{C}$ . Humidity inside the chamber was continuously monitored via a hygrometer [23]. Images were captured by using long distance lenses connected to a high-speed camera [24] with a  $2 \mu\text{s}$  minimum exposure time and 10 kHz maximum frame rate. The system was backlit by using a halogen lamp with fiber optic light guide and occasionally by an arc lamp. The liquids used for the stability experiments were glycerol and polyethylene oxide (PEO, 300 kDa) solutions which were prepared by addition of 2.5 M aqueous KCl solutions to pure glycerol or PEO dissolved in ethanol and water (1:1 by volume) to adjust the conductivity.

Liquid solutions were fed to the nozzle through a Teflon tubing using a syringe pump [25]. To avoid accumulation and keep the liquid level same as the electrode surface, liquid was drained at the same rate from the reservoir below the hole. The upper and lower electrodes were positioned such that the nozzle was centered in the hole on the bottom electrode. Upon application of sufficiently high potential (on the order of 1–6 kV) [26] between the electrodes, a thin jet was emitted from the tip of the “cone”. Flow rate and voltage were increased gradually while sustaining the cone-jet transition to avoid sudden dielectric breakdown. Current was monitored via an electrometer [27] in serial connection with the computer.

We studied the effect of electrode separation distance on the stability of jets through their centerline deflection [Fig. 1(a)]. Centerline deflection of short jets (at electrode separation: 5.5–6.75 mm range) at the lower electrode was compared to that of long jets (at electrode separation: 25.1 mm) at the same location with respect to the upper electrode [see inset in Fig. 1(a)]. When all other conditions

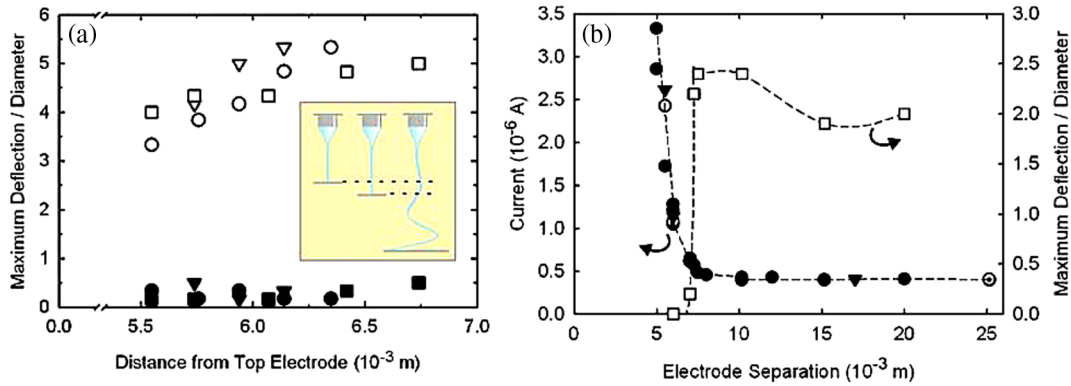


FIG. 1 (color online). (a) Comparison of centerline deflection of a jet at the deployment point on the bottom electrode produced with small electrode separations (solid symbols) vs the centerline deflection of a jet formed between 25.1 mm electrode separation (open symbols) at the equivalent position with respect to the nozzle (see inset). Data were determined from images of the PEO solution (conductivity:  $431 \mu\text{S}/\text{cm}$ ) jet under 1 ml/h flow rate and  $4119 \text{ V}/\text{cm}$  electric field. Maximum deflection of the jet refers to the largest horizontal length scanned by the jet within the captured images. (b) Variation of measured current and maximum deflection with electrode separation for PEO experiments done using different salts and nozzle materials. Solid circles: LiCl doped PEO solution ( $430 \mu\text{S}/\text{cm}$ ) with stainless steel needle; solid triangles: KCl doped PEO solution ( $431 \mu\text{S}/\text{cm}$ ) with stainless steel needle; open circles: KCl doped PEO solution ( $436 \mu\text{S}/\text{cm}$ ) with Teflon needle having copper wire connection; and open triangles: KCl doped PEO solution ( $428 \mu\text{S}/\text{cm}$ ) with copper coated needle.

were kept constant, the centerline deflection of the PEO jets decreased by an order of magnitude when the electrode separation was below  $\sim 7.2$  mm (Fig. 1). Coincident with this improvement in deflection stability, the total current measured between the parallel plate electrodes showed a sudden increase [Fig. 1(b)]. Current increased as a function of electrode separation irrespective of the type of ions in the solution or the nozzle material [28]. If the current between the parallel plate electrodes were carried only by the jet, deflections should have amplified at smaller electrode separations as the surface charge density is expected to increase with higher current [Fig. 1(b)]. These unexpected observations prompt us to raise two important questions: (i) Why is there a sudden increase in the current below a critical electrode separation? (ii) Why does the deflection stability improve significantly instead of getting worse?

Another manifestation of this contradiction is that the instability growth rates predicted by the existing theories [14,15] using the charge densities from total current are 3 orders of magnitude higher than the experimentally determined values. We determined the instability growth rates of a Newtonian liquid (glycerol) jet by using an image analysis program written in MATLAB [29]. Liquid conductivity and flow rate were adjusted such that the diameter of the jet was large enough to do accurate image analysis and the instability growth rate was small enough to capture clear images. Each disturbance wave was traced in time and changes in its amplitude were found by assuming that jet travels with the average velocity of the stream [Fig. 2(a)]. The change in the amplitude of the disturbances as a function of time [slope of line in Fig. 2(b)] gives the temporal growth rate of the disturbances as  $5213 \text{ s}^{-1}$ . On

the other hand, when the instability growth rate is calculated from the theory proposed by Saville [14] using the radial electric field estimated from the total measured current, the temporal growth rate is found as  $\sim 1.2 \times 10^6 \text{ s}^{-1}$ , a value that is nearly 3 orders of magnitude higher.

To explain the unexpected observations described above, we focus our attention on the current behavior.

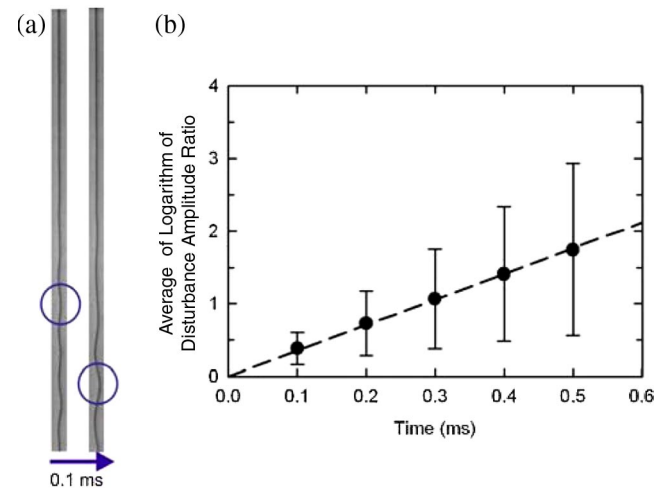


FIG. 2 (color online). Experimental determination of temporal instability growth rate for glycerol. 150 images of the jet are captured at 10 000 fps and  $2 \mu\text{s}$  exposure time in each electrode separation. Using a MATLAB program, the centerline of the jet is located and its deflection from vertical is found in every image. Each disturbance wave is traced in time and changes in its amplitude are determined by assuming that it is convected downstream with the average velocity of the stream. (a) Representative images from one of the experiments. (b) Variation of amplitude of disturbances as a function of time.

There are two possible mechanisms that can introduce charged species to the gas and cause sudden increase in the current: gas ionization [30] and ion emission from the jet [31]. In order to understand the requirements for gas ionization, we consider the conservation of the electrons for convection dominated systems [32]:

$$\frac{1}{r} \frac{\partial}{\partial r} (r n_e v_{e,r}) \sim |v_e| \alpha n_e. \quad (1)$$

Here,  $r$ ,  $n_e$ , and  $v_e$  are the radial coordinate, number density of the electrons, and velocity of the electrons, respectively.  $\alpha$  is the Townsend coefficient,  $\alpha = AP \exp(-BP/E)$  [33], where  $P$  is the pressure and  $A$  and  $B$  are constants specific to the gas. Requirement for the change in convection to scale equally as generation in Eq. (1) provides the criteria for the electric field and length scale as  $E \sim BP$  and  $L_r \sim 1/AP$ , respectively. According to the first criterion, the electric field should be  $\sim 2.77 \times 10^7$  V/m for ionization of air under atmospheric pressure. The electric field at the liquid surface scales as  $E_n \sim (2\gamma/\epsilon_0 r)^{1/2}$  [34], where  $\gamma$ ,  $\epsilon_0$ , and  $R$  are the surface tension of the liquid, vacuum permittivity, and the radial position of the interface, respectively. Based on the normal electric field, ionization is expected to take place somewhere close to the end of the “cone” region ( $R < 19 \mu\text{m}$ ) in our experiments with glycerol. Although high enough to cause ionization, normal electric field around the cone is not sufficient to cause ion emission, which requires  $\sim 10^9$  V/m [31]. Hence, we conclude that the most likely explanation for the increase in current is gas ionization. Using the second criterion length scale for the “ionization zone” is  $L_r \sim 0.9 \mu\text{m}$  for the case of air. This length scale is much less than other length scales in the system, such as the radius of the jet and the nozzle diameter; thus we conclude that the effect of ionization is rather local.

We considered the role of gas ionization by changing the composition of the gas. Figure 3 shows representative snapshots from experiments at two different gas compositions for a glycerol solution (with a conductivity of  $19.5 \mu\text{S/cm}$ ) flowing at 12 ml/h rate and under a 943 V/mm electric field. Under otherwise identical conditions, either decreasing the electrode separation [Fig. 3(a)] or increasing the humidity [Fig. 3(c)] decreased the amplitude of the disturbances on the jet and increased the length of the “straight segment” of the jet. As shown above, electric field normal to the liquid surface becomes high enough to initiate ionization close to the end of the cone. Therefore, around this region electrons multiply in number and generate positively charged ions while moving towards the cone and the jet. Upon reaching the air-liquid interface, electrons partially neutralize the surface charge. The reduction in the surface charge density of the jet leads to the observed decrease in the instability growth rate and diminishes ionization below the region of neutralization. Generated ions contribute to the total current by reaching

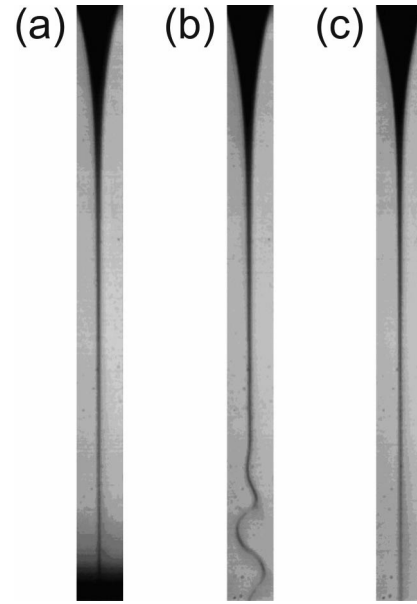


FIG. 3. Representative images for glycerol solution filaments at: (a) electrode separation = 8 mm, relative humidity =  $25 \pm 0.1\%$ , current =  $5.46 \mu\text{A}$ ; (b) electrode separation = 16 mm, relative humidity =  $25 \pm 0.1\%$ , current =  $5.2 \mu\text{A}$ ; and (c) electrode separation = 16 mm, relative humidity =  $70 \pm 0.1\%$ , current =  $7.8 \mu\text{A}$ .

the lower electrode. Hence, as the jet stabilized the current increased significantly [from 5.2 to  $7.8 \mu\text{A}$  for Fig. 3(b) and 3(c)]. Doping the atmosphere with argon gas also provided the same behavior as increasing the humidity of the air.

To provide further evidence for gas ionization, we measured the current through the air and the jet independently by insulating the pool at the center of the bottom electrode from the rest of the electrode. Current measurements from electrometers connected in series to the pool and the rest of the bottom electrode showed that there was indeed a significantly higher current through the air. For example, the current outside of the pool and through the pool at 65% relative humidity was 0.98 and  $0.56 \mu\text{A}$ , respectively, when using a glycerol solution with a conductivity of  $6.8 \mu\text{S/cm}$ , at 9.52 mm electrode separation, 7920 V, and 2 ml/h flow rate. The current through the air also increased as a function of humidity, confirming the results shown in Figs. 3(b) and 3(c). Hence, it is confirmed that in the presence of ionization, current measured between electrodes has contributions other than the current carried by the jet. Unless this contribution is taken into account, surface charge density of the jet will be over estimated, causing an apparent discrepancy between the observed and estimated instability growth rates, as pointed out at the beginning.

These observations show that the stability of the jet is improved through partial neutralization of surface charge by the electrons produced by gas ionization. Upon chang-

ing the surrounding gas with one that ionizes more readily, or increasing the radial electric field, ionization and gas discharge can be enhanced. As the electrode separation decreases, existence of the nozzle and the cone enhances the local electric field causing enhancement in the radial electric field [35]. Enhanced ionization at small separations also explains the sudden increase in the current as a function of electrode separation [Fig. 1(b)]. The contribution of other stabilization mechanisms at small electrode separations, such as pinning of the end of the jet by capillary or viscous forces or wavelength selection is negligible [35]. More importantly, none of these alternative mechanisms can explain the current behavior.

It should also be noted that the rate at which radial electric field around the jet decays depends on the radius of the jet. Thus, the number of gas ions generated is a function of radius and initial charge density of the jet. When the jet is too thin or the initial charge density is not large enough, effects of ionization and hence the effects of electrode separation are not expected to be significant. A discussion on the effect of divergence of the electric field on corona discharges around EHD jets can be found in Borra *et al.* [22].

Financial support for this work was provided by ARO-MURI under Grant No. W911NF-04-1-0170, MRSEC No. NSF/DMR-0213706, and the NASA University Research, Engineering and Technology Institute on Bio Inspired Materials (BIMat, Grant No. NCC-1-02037).

\*Deceased.

†Corresponding author.

- [1] J. Zeleny, *Phys. Rev.* **10**, 1 (1917).
- [2] G. I. Taylor, *Proc. R. Soc. A* **313**, 453 (1969).
- [3] A. L. Huebner, *J. Fluid Mech.* **38**, 679 (1969).
- [4] J. B. Fenn, M. Mann, C. K. Meng, S. K. Wong, and C. Whitehouse, *Science* **246**, 64 (1989).
- [5] A. Formhals, U.S. Patent No. 1 975 504 (1934).
- [6] H. F. Poon, Ph.D. thesis, Princeton University, 2002.
- [7] C.-H. Chen, D. A. Saville, and I. A. Aksay, *Appl. Phys. Lett.* **88**, 154104 (2006).
- [8] C.-H. Chen, D. A. Saville, and I. A. Aksay, *Appl. Phys. Lett.* **89**, 124103 (2006).
- [9] J. Kameoka, R. Orth, Y. Yang, D. Czaplewski, R. Mathers, G. W. Coates, and H. G. Craighead, *Nanotechnology* **14**, 1124 (2003).
- [10] D. A. Czaplewski, J. Kameoka, R. Mathers, G. W. Coates, and H. G. Craighead, *Appl. Phys. Lett.* **83**, 4836 (2003).
- [11] H. Liu, J. Kameoka, D. A. Czaplewski, and H. G. Craighead, *Nano Lett.* **4**, 671 (2004).
- [12] D.-Y. Lee, Y.-S. Shin, S.-E. Park, T.-U. Yu, and J. Hwang, *Appl. Phys. Lett.* **90**, 081905 (2007).
- [13] D. Sun, C. Chang, S. Li, and L. Lin, *Nano Lett.* **6**, 839 (2006).
- [14] D. A. Saville, *Phys. Fluids* **14**, 1095 (1971).
- [15] M. M. Hohman, M. Shin, G. Rutledge, and M. P. Brenner, *Phys. Fluids* **13**, 2201 (2001).
- [16] D. H. Reneker, A. L. Yarin, H. Fong, and S. Koombhongse, *J. Appl. Phys.* **87**, 4531 (2000).
- [17] M. M. Hohman, M. Shin, G. Rutledge, and M. P. Brenner, *Phys. Fluids* **13**, 2221 (2001).
- [18] A. M. Ganan-Calvo, J. Davila, and A. Barrero, *J. Aerosol Sci.* **28**, 249 (1997).
- [19] K. Tang and A. Gomez, *J. Colloid Interface Sci.* **175**, 326 (1995).
- [20] A. Jaworek and A. Krupa, *J. Electrostat.* **40**, 173 (1997).
- [21] M. Cloupeau, *J. Aerosol Sci.* **25**, 1143 (1994).
- [22] J. P. Borra, Y. Tombette, and P. Ehouarn, *J. Aerosol Sci.* **30**, 913 (1999).
- [23] Control Company, 308 West Edgewood, Friendswood, TX.
- [24] Model Motion Pro, Redlake, San Diego, CA.
- [25] Model Harvard 33 Twin Syringe Pump, Harvard Apparatus, Holliston, MA.
- [26] Model 620A, Trek Inc., Beaverton, OR.
- [27] Model 6514, Keithley, Cleveland, OH.
- [28] The type of nozzle was changed only to make sure that it does not change the current. In all the other experiments stainless steel nozzles were used.
- [29] MATLAB version 6.5.0.180913a (release 13), Image Analysis Toolbox version 3.2, The MathWorks Inc., Natick, MA.
- [30] J. S. Townsend, *Philos. Mag.* **1**, 198 (1901).
- [31] J. V. Iribarne and B. A. Thomson, *J. Chem. Phys.* **64**, 2287 (1976).
- [32] Peclet number, i.e., the ratio of the convective to diffusive mass transport, for the electrons above the critical electric field for ionization is  $\sim 1000$ . Therefore convection is the dominant mass transfer mechanism in our system.
- [33] J. D. Cobine, *Gaseous Conductors* (Dover Publications, Inc., New York, 1958).
- [34] G. I. Taylor, *Proc. R. Soc. A* **280**, 383 (1964).
- [35] S. Korkut, D. A. Saville, and I. A. Aksay (to be published).